

# Magnetic Excitations in quasi two-dimensional Spin-Peierls Systems

Wolfram Brenig

*Institut für Theoretische Physik, Universität zu Köln Zùlpicher Str. 77, 50937 Köln, Germany*

(May 6, 2017)

A study is presented of a two-dimensional frustrated and dimerized quantum spin-system which models the effect of inter-chain coupling in a spin-Peierls compound. Employing a bond-boson method to account for quantum disorder in the ground state the elementary excitations are evaluated in terms of gapful triplet modes. Results for the ground state energy and the spin gap are discussed. The triplet dispersion is found to be in excellent agreement with inelastic neutron scattering data in the dimerized phase of the spin-Peierls compound CuGeO<sub>3</sub>. Moreover, consistent with these neutron scattering experiments, the low-temperature dynamic structure factor exhibits a high-energy continuum split off from the elementary triplet mode.

PACS: 75.10.Jm, 75.40.Gb, 78.70.Nx

## I. INTRODUCTION

The recent discovery of the anorganic spin-Peierls compounds CuGeO<sub>3</sub> [1] and  $\alpha'$ -NaV<sub>2</sub>O<sub>5</sub> [2,3] has greatly stimulated interest in low-dimensional magnetism. While many properties of these novel materials can be described in terms of quasi *one*-dimensional (1D) quantum spin-systems, clear evidence for a substantial degree of *two*-dimensionality (2D) of their magnetism has been found – most noteworthy by inelastic neutron scattering (INS) which displays a sizeable transverse dispersion of the magnetic excitations in CuGeO<sub>3</sub> [4–6]. In the present study I will establish a simple framework to interpret the spin dynamics of a frustrated and dimerized 2D quantum spin-model with a particular focus on the low-temperature phase of CuGeO<sub>3</sub>.

CuGeO<sub>3</sub> is an anorganic spin-Peierls system with a lattice dimerization transition at a temperature  $T_{SP} \simeq 14K$  [1,4–8]. Its structure comprises of weakly coupled CuO<sub>2</sub> chains along the *c*-axis, with copper in a spin-1/2 state [9,10]. The nearest-neighbor (*n.n.*) exchange-coupling between copper spins along the CuO<sub>2</sub> chains is strongly reduced by almost orthogonal intermediate oxygen states [11]. Therefore, next-nearest-neighbor (*n.n.n.*) exchange in CuGeO<sub>3</sub> is relevant. Both, *n.n.* and *n.n.n.* exchange, are antiferromagnetic (AFM) [11,12] implying intra-chain frustration. In addition, *n.n.*, as well as *n.n.n.* inter-chain exchange is present which proceeds via the O2 sites [11,13]. This exchange is believed to be one order of magnitude less than the intra-chain coupling [4–6,11,13] and comparable to  $T_{SP}$ . Therefore the inter-chain coupling should be relevant in the dimerized

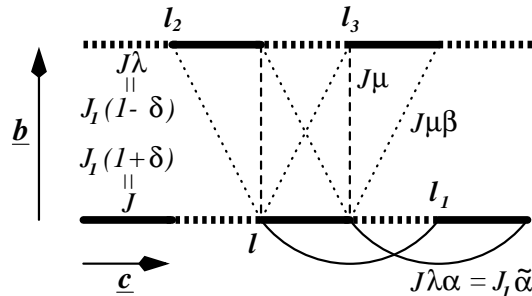


FIG. 1. The  $J$ - $\lambda$ - $\alpha$ - $\mu$ - $\beta$  model. Line segments refer to exchange couplings for spins located at segment vertices. Inter-chain couplings are shown for a single dimer site only.  $\mathbf{b} = b\mathbf{e}_b$  and  $\mathbf{c} = c\mathbf{e}_c$  are the primitive vectors.

phase. This may be a key element in the INS [4–7] and magnetic Raman scattering [14–16] data.

A minimal model of CuGeO<sub>3</sub> which includes intra-, as well as inter-chain interactions is the  $J$ - $\lambda$ - $\alpha$ - $\mu$ - $\beta$  model [11,17] depicted in fig. 1. The various line segments label the coupling strengths  $J$ ,  $J\lambda$ ,  $J\lambda\alpha$ ,  $J\mu$ , and  $J\mu\beta$  between the spins located at the vertices in this figure.  $J$  refers to the ‘strongest’ or dimer-bond the left vertices of which form the dimer lattice  $\mathbf{l} \in \mathcal{D}$ . Most important the dimerization in fig. 1 is staggered along the *b*-axis. This is realized both, in CuGeO<sub>3</sub> [10] as well as in  $\alpha'$ -NaV<sub>2</sub>O<sub>5</sub> [18], and turns out to be relevant for the magnon dispersion. In fig. 1 an additional, so-called ‘natural’ labeling of the intra-chain parameters is introduced, i.e.  $J_1$ ,  $\tilde{\alpha}$ , and  $\delta$ . This notation is frequently used in the context of the 1D dimerized and frustrated spin-chain limit. In CuGeO<sub>3</sub>  $J_1$  is approximately 160K [19,20]. Consensus on the precise magnitude of the intra-chain frustration-ratio  $\tilde{\alpha}$  is still lacking. Studies of the magnetic susceptibility, which has been compared only to 1D models, have resulted in  $\tilde{\alpha} \approx 0.24$  [19] as well as in  $\tilde{\alpha} \approx 0.35$  [20]. This would place CuGeO<sub>3</sub> in the vicinity of the critical value  $\tilde{\alpha}_c \simeq 0.2411$  for the opening of a spin gap solely due to frustration [21].  $\delta$  resembles the lattice dimerization which is finite for  $T < T_{SP}$  only. Values for the zero-temperature dimerization  $\delta(T=0)$  ranging from 0.21 to 0.012 have been suggested [11,19,20,22]. Knowledge on the magnitude of  $\mu$  and  $\mu\beta$  is limited to  $|\mu|, |\mu\beta| \ll 1$  [11,13].

Magnetic excitations in CuGeO<sub>3</sub> are clearly distinct among the uniform (U), i.e.  $T > T_{SP}$ , and the dimerized (D), i.e.  $T < T_{SP}$ , phase. While the dynamic structure factor exhibits a gapless, *c*-axis dispersive two-spinon continuum similar to that of the 1D Heisenberg chain above  $T_{SP}$  [23], well defined magnon-like excitations with

sizeable c- and b-axis dispersion have been observed below  $T_{SP}$  [4–6,24]. These magnons are gapful and are split off from a continuum which, at zone-center, starts at roughly twice the magnon gap [24–26,17].

The aim of this work is to study the magnetic properties of the  $J$ - $\lambda$ - $\alpha$ - $\mu$ - $\beta$  model with a focus on the D-phase of  $\text{CuGeO}_3$ . First I will describe a bond-spin representation of the  $J$ - $\lambda$ - $\alpha$ - $\mu$ - $\beta$  model which, in turn, is treated by an appropriate linearization. Next, results for the ground state energy, the spin gap, the magnon dispersion, and the dynamic structure factor are contrasted against other theoretical approaches and are compared with experimental findings. Finally, details of an alternative mean-field approach using the bond-spin representation are provided in appendix A.

## II. BOND-OPERATOR THEORY

In this section the properties of the  $J$ - $\lambda$ - $\alpha$ - $\mu$ - $\beta$  model are discussed by representing the *site*-spin algebra in terms of *bond*-spin operators [27]. First, the essential features of these operators are briefly restated. Consider any two spin-1/2 operators  $\mathbf{S}_1$  and  $\mathbf{S}_2$ . The eigenstates of the related total spin are a singlet  $|s\rangle$  and three triplets  $|t_\alpha\rangle$  with  $\alpha = x, y, z$ . These can be created out of a vacuum  $|0\rangle$  by applying the bosonic operators  $s^\dagger$  and  $t_\alpha^\dagger$

$$\begin{aligned} s^\dagger |0\rangle &\hat{=} |s\rangle = (|\uparrow\downarrow\rangle - |\downarrow\uparrow\rangle)/\sqrt{2} \\ t_x^\dagger |0\rangle &\hat{=} |t_x\rangle = -(|\uparrow\uparrow\rangle - |\downarrow\downarrow\rangle)/\sqrt{2} \\ t_y^\dagger |0\rangle &\hat{=} |t_y\rangle = i(|\uparrow\uparrow\rangle + |\downarrow\downarrow\rangle)/\sqrt{2} \\ t_z^\dagger |0\rangle &\hat{=} |t_z\rangle = (|\uparrow\downarrow\rangle + |\downarrow\uparrow\rangle)/\sqrt{2} \end{aligned} \quad (1)$$

where  $[s, s^\dagger] = 1$ ,  $[s^{(\dagger)}, t_\alpha^{(\dagger)}] = 0$ , and  $[t_\alpha, t_\beta^\dagger] = \delta_{\alpha\beta}$ . The action of  $\mathbf{S}_1$  and  $\mathbf{S}_2$  on this space leads to the representation

$$S_1^\alpha \hat{=} \frac{1}{2}(\pm s^\dagger t_\alpha \pm t_\alpha^\dagger s - i\varepsilon_{\alpha\beta\gamma} t_\beta^\dagger t_\gamma) \quad (2)$$

for the individual spin operators. Here  $\varepsilon_{\alpha\beta\gamma}$  is the Levi-Civita symbol and a summation over repeated indices is implied hereafter. The upper(lower) subscript on the lhs. of (2) refer to upper(lower) sign on the rhs.. The bosonic Hilbert space has to be restricted to the physical Hilbert space, i.e. either one singlet or one triplet, by the constraint

$$s^\dagger s + t_\alpha^\dagger t_\alpha = 1 \quad (3)$$

Using (2) and (3) it is simple to check, that  $\mathbf{S}_1$  and  $\mathbf{S}_2$  satisfy a spin algebra indeed and moreover that

$$S_1^\alpha S_2^\alpha = -\frac{3}{4}s^\dagger s + \frac{1}{4}t_\alpha^\dagger t_\alpha \quad (4)$$

In order to transform the  $J$ - $\lambda$ - $\alpha$ - $\mu$ - $\beta$  model into the boson representation a particular distribution 'I' of bonds, i.e. pairs of spins  $\mathbf{S}_{11}$  and  $\mathbf{S}_{12}$ , has to be selected. Here

this selection will be based on the limit of strong dimerization  $(\lambda, \lambda\alpha) \rightarrow (0, 0)$ , or equivalently  $(\tilde{\alpha}, \delta) \rightarrow (0, 1)$ , and small inter-chain coupling  $(\mu, \mu\beta) \rightarrow (0, 0)$ . In this limit the ground state is a product of singlets on each dimer-bond while the elementary excitations are composed of the corresponding localized triplets. Therefore it is natural to place the singlet and triplet bosons onto the dimer bonds, i.e.  $\mathbf{S}_{11} = \mathbf{S}_1$  and  $\mathbf{S}_{12} = \mathbf{S}_{1+c}$  with  $\mathbf{l} \in \mathcal{D}$ . The transformed Hamiltonian reads

$$\begin{aligned} H &= H_0 + H_1 + H_2 + H_3 \\ H_0 &= \sum_{\mathbf{l} \in \mathcal{D}} \left( -\frac{3}{4}s_1^\dagger s_1 + \frac{1}{4}t_{1\alpha}^\dagger t_{1\alpha} \right) \\ H_1 &= \sum_{\mathbf{l} \neq \mathbf{m} \in \mathcal{D}} a(\mathbf{l}, \mathbf{m}) (t_{1\alpha}^\dagger t_{\mathbf{m}\alpha} s_{\mathbf{m}}^\dagger s_1 + t_{1\alpha}^\dagger t_{\mathbf{m}\alpha}^\dagger s_{\mathbf{m}} s_1 + h.c.) \\ H_2 &= \sum_{\mathbf{l} \neq \mathbf{m} \in \mathcal{D}} b(\mathbf{l}, \mathbf{m}) (i\varepsilon_{\alpha\beta\gamma} t_{\mathbf{m}\alpha}^\dagger t_{1\beta}^\dagger t_{1\gamma} s_{\mathbf{m}} + h.c.) \\ H_3 &= \sum_{\mathbf{l} \neq \mathbf{m} \in \mathcal{D}} c(\mathbf{l}, \mathbf{m}) (t_{1\alpha}^\dagger t_{\mathbf{m}\alpha}^\dagger t_{\mathbf{m}\beta}^\dagger t_{1\beta} - t_{1\alpha}^\dagger t_{\mathbf{m}\beta}^\dagger t_{\mathbf{m}\alpha}^\dagger t_{1\beta}) \quad , \end{aligned} \quad (5)$$

where each local Hilbert space is subject to the constraint (3) and, if not explicitly stated otherwise, the unit of energy is  $J$  hereafter. The inter-dimer matrix elements can be obtained from fig. 1

$$\begin{aligned} a(\mathbf{l}, \mathbf{m}) &= -\frac{1}{4}[t_1\delta_{\mathbf{m}\mathbf{l}_1} + t_2(\delta_{\mathbf{m}\mathbf{l}_2} + \delta_{\mathbf{m}\mathbf{l}_3})] \\ b(\mathbf{l}, \mathbf{m}) &= \frac{1}{4}[\lambda(\delta_{\mathbf{l}\mathbf{l}_1} - \delta_{\mathbf{m}\mathbf{l}_1}) + \mu(\delta_{\mathbf{m}\mathbf{l}_3} - \delta_{\mathbf{m}\mathbf{l}_2} + \delta_{\mathbf{l}\mathbf{l}_2} - \delta_{\mathbf{l}\mathbf{l}_3})] \\ c(\mathbf{l}, \mathbf{m}) &= -\frac{1}{4}[t_3\delta_{\mathbf{m}\mathbf{l}_1} + t_4(\delta_{\mathbf{m}\mathbf{l}_2} + \delta_{\mathbf{m}\mathbf{l}_3})] \quad , \end{aligned} \quad (6)$$

where  $\mathbf{l}_{1,2,3}$  are defined in fig. 1 and  $t_1 = \lambda(1 - 2\alpha)$ ,  $t_2 = \mu(1 - 2\beta)$ ,  $t_3 = \lambda(1 + 2\alpha)$ , and  $t_4 = \mu(1 + 2\beta)$ . As anticipated, the inter-dimer matrix elements  $a(\mathbf{l}, \mathbf{m})$ ,  $b(\mathbf{l}, \mathbf{m})$ , and  $c(\mathbf{l}, \mathbf{m})$  vanish in the strong dimer limit leaving the Hamiltonian diagonal in  $s_1$  and  $t_{1\alpha}$ .

In order to treat the local constraint and the dimer interactions approximations have to be made. To this end I will employ the Holstein-Primakoff (HP) representation of the bond-operators which has been detailed in [28–30]. In this representation the constraint is treated by eliminating the singlet operator via  $s_1^\dagger = s_1 = (1 - t_{1\alpha}^\dagger t_{1\alpha})^{-1/2}$ . Moreover, after inserting this into the Hamiltonian only terms up to second order in the triplet operators are retained. The latter procedure is analogous to the linear spin-wave approximation in systems with broken spin-rotational invariance. The linearized (LHP) Hamiltonian is given by

$$\begin{aligned} H_{LHP} &= -\frac{9}{4}D \\ &+ \frac{1}{2} \sum_{\mathbf{k} \in \mathcal{B}} \Psi_{\mathbf{k}\alpha}^\dagger \begin{bmatrix} 1 + \epsilon_{\mathbf{k}} & \epsilon_{\mathbf{k}} \\ \epsilon_{\mathbf{k}} & 1 + \epsilon_{\mathbf{k}} \end{bmatrix} \Psi_{\mathbf{k}\alpha} \end{aligned} \quad (7)$$

$$\epsilon_{\mathbf{k}} = -\frac{1}{2}[t_1 \cos(2k_c) + 2t_2 \cos(k_b) \cos(k_c)] \quad , \quad (8)$$

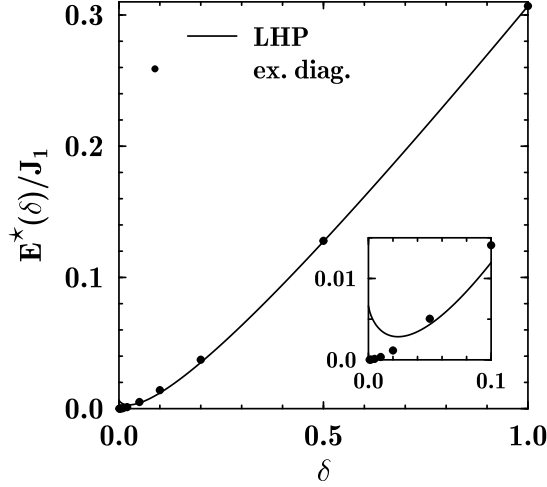


FIG. 2. Ground state energies in the dimerized-chain limit: LHP-theory (solid) versus exact diagonalization [31] (solid dots), errors are less than marker size. Inset: small  $\delta$  limit.  $E^*(\delta)/J_1 = -[(1+\delta)E_g((1-\delta)/(1+\delta), 0) - E_g^{Bethe}]$ .

where  $D$  is the number of dimers and  $\mathbf{k}$  is a momentum vector restricted to a Wigner-Seitz cell  $\mathcal{B}$  of the reciprocal lattice. For comparison with experimental data  $\mathcal{B}$  is oriented with respect to the non-dimerized system, instead of the Brillouin zone of the dimer lattice, i.e.  $\mathbf{k} = (k_b, k_c)$  with  $bk_b = 0 \dots 2\pi$  and  $ck_c = 0 \dots \pi$  with  $b, c$  set to unity hereafter.  $\Psi_{\mathbf{k}\alpha}^{(\dagger)}$  is a spinor with  $\Psi_{\mathbf{k}\alpha}^\dagger = [t_{\mathbf{k}\alpha}^\dagger \ t_{-\mathbf{k}\alpha}]$  and  $t_{1\alpha}^\dagger = 1/\sqrt{D} \sum_{\mathbf{k}} e^{-i\mathbf{k} \cdot \mathbf{l}} t_{\mathbf{k}\alpha}^\dagger$ .

Eqn. (7) describes a threefold degenerate set of dispersive triplets. The triplets are renormalized by ground-state quantum-fluctuations. These are produced by the terms of type  $t_{\mathbf{k}\alpha}^\dagger t_{-\mathbf{k}\alpha}^\dagger$  and their hermitian conjugate. The excitation spectrum  $E_{\mathbf{k}}$  follows from a Bogoliubov transformation

$$H_{LHP} = -\frac{9}{4}D + \sum_{\mathbf{k} \in \mathcal{B}, \alpha} E_{\mathbf{k}} (a_{\mathbf{k}\alpha}^\dagger a_{\mathbf{k}\alpha} + \frac{1}{2}) \quad (9)$$

$$E_{\mathbf{k}} = \sqrt{1 + 2\epsilon_{\mathbf{k}}} \quad , \quad (10)$$

where  $a_{\mathbf{k}\alpha}^{(\dagger)}$  are the Bogoliubov quasi-particles which are given by

$$\Psi_{\mathbf{k}\alpha} = \begin{bmatrix} g_{\mathbf{k}} & h_{\mathbf{k}} \\ h_{\mathbf{k}} & g_{\mathbf{k}} \end{bmatrix} \Phi_{\mathbf{k}\alpha} \quad (11)$$

$$h_{\mathbf{k}}^2 = \frac{1}{2} \left( \frac{1 + \epsilon_{\mathbf{k}}}{E_{\mathbf{k}}} - 1 \right) \quad ; \quad h_{\mathbf{k}} g_{\mathbf{k}} = -\frac{1}{2} \frac{\epsilon_{\mathbf{k}}}{E_{\mathbf{k}}}$$

$$g_{\mathbf{k}}^2 = \frac{1}{2} \left( \frac{1 + \epsilon_{\mathbf{k}}}{E_{\mathbf{k}}} + 1 \right) \quad ,$$

where  $\Phi_{\mathbf{k}\alpha}^{(\dagger)}$  is a spinor with  $\Phi_{\mathbf{k}\alpha}^\dagger = [a_{\mathbf{k}\alpha}^\dagger \ a_{-\mathbf{k}\alpha}]$ .

To conclude this section, I note that instead of treating the constraint by means of the HP representation one may also apply the so called bond-operator mean-field

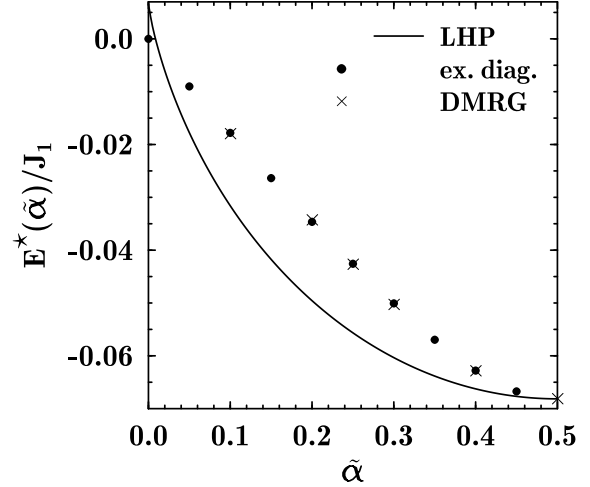


FIG. 3. Ground state energies in the frustrated-chain limit: LHP-theory (solid) versus exact diagonalization [32] (solid dots), and DMRG [33] (crosses), errors are less than marker size.  $E^*(\alpha)/J_1 = -[E_g((1-2\alpha), 0) - E_g^{Bethe}]$ .

theory (MFT) of [27]. The application of this method to the  $J$ - $\lambda$ - $\alpha$ - $\mu$ - $\beta$  model is detailed in appendix A. As will become evident in section III B this technique seems less well suited in the present context.

### III. RESULTS

In the following sections the consequences of the LHP representation of the 2D  $J$ - $\lambda$ - $\alpha$ - $\mu$ - $\beta$  model will be contrasted against other known results in the limiting case of the 1D  $J_1$ - $\tilde{\alpha}$ - $\delta$  model as well as INS data observed on  $\text{CuGeO}_3$ .

#### A. Ground State Energy

From (9) it is obvious, that the ground state energy per lattice site,  $E_g$ , is equal to  $-3/8$  at the point of complete dimerization. This is the proper energy gain for a bare singlet formation. For arbitrary  $t_1$  and  $t_2$

$$E_g(t_1, t_2) = -\frac{9}{8} + \frac{3}{2\pi^2} \int_0^\pi dk_c \{ [1 - 2t_2 \cos(k_c) - t_1 \cos(2k_c)]^{-1/2} \mathbf{E} \left( \frac{-4t_2 \cos(k_c)}{1 - 2t_2 \cos(k_c) - t_1 \cos(2k_c)} \right) \} \quad (12)$$

where  $\mathbf{E}$  is the complete elliptic integral of the second kind. For vanishing inter-chain coupling this simplifies to

$$E_g(t_1, 0) = -9/8 + \frac{3}{2\pi} \sqrt{1 - t_1} \mathbf{E} \left( \frac{2t_1}{t_1 - 1} \right) \quad , \quad (13)$$

which can be compared to existing results in various regions of the  $(\tilde{\alpha}, \delta)$ -plane of the frustrated and dimerized

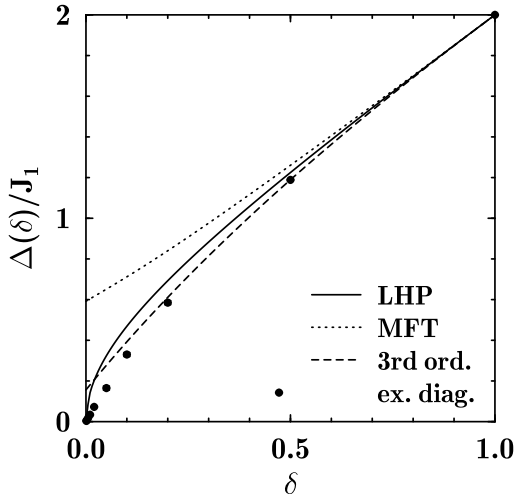


FIG. 4. Spin gaps in the dimerized-chain limit: LHP-theory (solid) versus 3rd-order perturbation theory [17,34] (dashed), MFT (dotted), and exact diagonalization [31] (solid dots), errors are less than marker size.

spin-1/2 chain. In particular at the isotropic Heisenberg point, i.e.  $(\tilde{\alpha}, \delta) = (0, 0)$ ,  $E_g = 3/(\sqrt{2}\pi) - 9/8 \approx -0.4498$  which agrees reasonably well with the Bethe Ansatz result  $E_g^{Bethe} = 1/4 - \ln(2) \approx -0.4431$ . In fig. 2 the ground state energy along the  $(\tilde{\alpha} = 0, \delta)$ -line, i.e. for a dimerized chain, is contrasted against results from exact diagonalization [31]. Deviations are within the numerical error of the diagonalization data for  $\delta \gtrsim 0.05$ . For dimerizations below 0.05 small differences are caused by an unphysical extremum in the LHP energy which is visible in the inset. While the agreement is encouraging along the  $(\tilde{\alpha} = 0, \delta)$ -line, only qualitative consistency is to be expected along the  $(\tilde{\alpha}, \delta = 0)$ -line since this region is more distant from the strong dimer limit  $(\tilde{\alpha}, \delta) \sim (0, 1)$ . This is shown in fig. 3 which compares  $E_g(\tilde{\alpha})$  with exact diagonalization [32] and density-matrix renormalization group (DMRG) [33] data for the case of a frustrated chain. This figure demonstrates that the LHP approach overestimates the frustration induced loss of ground state energy at intermediate  $\tilde{\alpha}$ .

### B. Spin Gap

The LHP approximation does not break the spin-rotational invariance and leaves the system in a quantum-disordered ground state. This is consistent with a spin gap  $\Delta$  of the triplet dispersion which, for positive  $t_1$  and  $t_2$ , is given by  $\Delta = \sqrt{1 - t_1 - 2t_2}$  and is situated at  $\mathbf{k} = (0, 0)$  and  $(\pi, \pi)$ . If  $t_1$  and  $t_2$  are such that the triplet modes turn massless, i.e.  $\Delta = 0$ , a quantum phase-transition towards antiferromagnetism (AFM) will occur at  $T = 0$ . In terms of  $\tilde{\alpha}$  and  $\delta$ , the AFM instability-line is located at  $\tilde{\alpha} + \delta = t_2(1 + \delta)$ . Beyond this line the LHP approach breaks down.

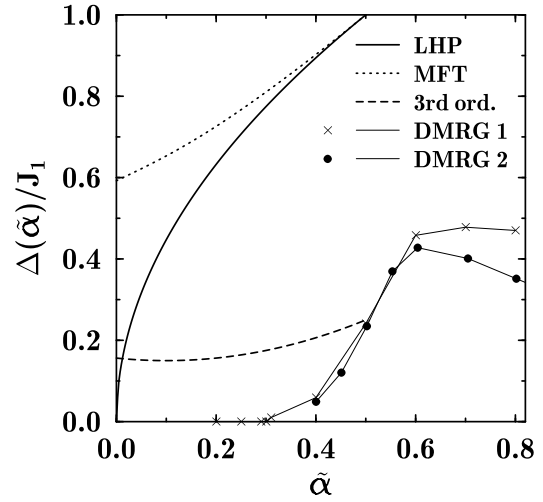


FIG. 5. Spin gaps in the frustrated-chain limit: LHP-theory (solid) versus 3rd-order perturbation theory [17] (dashed), MFT (dotted), and two DMRG calculations [33] (crosses), and [36] (solid dots), errors are less than marker size.

Next the LHP spin gap at  $t_2 = 0$  is compared to known results for the frustrated and dimerized spin-1/2 chain. In fig. 4  $\Delta(\delta)$  is contrasted against findings of exact diagonalization [31], perturbation theory up to third order in  $\lambda$  [17,34], and a solution of the MFT equations (A5–A7) which are discussed in appendix A. This figure displays reasonable agreement between the first three of these approaches for all values of  $\delta$ . In addition it shows that the MFT suffers from the inability to close the spin gap at the isotropic Heisenberg point [37,38]. This caveat renders the MFT unsuitable for the case of a systems with nearly massless spin excitations, e.g.  $\text{CuGeO}_3$ .

As noted in the previous section, analytic approaches based on the strong dimer limit are less reliable if considered along the  $(\tilde{\alpha}, \delta = 0)$ -line. Nevertheless, a comparison of  $\Delta(\tilde{\alpha})$  as obtained from the LHP theory with various other techniques is instructive and is shown in fig. 5. Qualitatively, all analytic methods depicted exhibit a tendency of the spin gap to increase as  $\tilde{\alpha}$  increases [35] however agreement with the DMRG data [33,36] is absent. In particular, while 3rd-order perturbation theory and MFT show no critical frustration-ratio  $\tilde{\alpha}_c$  and have a finite gap for all  $0 < \tilde{\alpha} < 0.5$  the LHP representation leads to a critical frustration-ratio  $\tilde{\alpha}_c = 0$ . Quite remarkably there are also substantial differences between the two DMRG results for  $\tilde{\alpha} \gtrsim 0.5$  [39].

### C. Triplet Dispersion

In this section the relevance of the model with respect to the spin excitations in  $\text{CuGeO}_3$  will be assessed by comparison of  $E_{\mathbf{k}}$  with INS data for the D-phase. In particular the role of two-dimensionality will be consid-

ered. The essential effect of a finite hopping amplitude  $t_2$  is a *mixing* of the b- and c-axis dispersion. This mixing is due to the staggering of the dimerization along the b-axis and leads to the  $t_2 \cos(k_b) \cos(k_c)$ -term in  $\epsilon_{\mathbf{k}}$ . Thus,  $E_{\mathbf{k}}$  involves terms of different periodicity in  $k_c$ , i.e.  $\cos(2k_c)$  and  $\cos(k_c)$ . Therefore, in contrast to the quasi 1D case, the degeneracy of the triplets at the momenta  $(0,0)$  and  $(0,\pi)$  is lifted. An identical reasoning based on the first-order contribution of a 3rd-order perturbation theory has been given in [17]. Expanding  $E_{\mathbf{k}}$  in terms of  $t_1$  and  $t_2$  I find agreement up to first order with the dispersion given in [17].

In fig. 6 INS data of the magnon dispersion in  $\text{CuGeO}_3$  are shown for momenta along the edges of the reciprocal lattice cell from  $\mathbf{k} = (0,0)$  to  $(0,\pi)$  as well as from  $(0,0)$  to  $(\pi/2,0)$  [6]. Although data exactly at  $(0,\pi)$  is lacking, it seems very likely from this figure that the triplet excitations in  $\text{CuGeO}_3$  are *not* degenerate at  $(0,0)$  and  $(0,\pi)$ . In order to demonstrate that the  $J$ - $\lambda$ - $\alpha$ - $\mu$ - $\beta$  model can account for the observed dispersion fig. 6 contains a comparison of  $E_{\mathbf{k}}$  with the INS data. Rather than performing this comparison by a least-square fit,  $E_{\mathbf{k}}$  has been identified with the magnon energies only at  $\mathbf{k} = (0,0)$ ,  $(0,\pi/2)$ , and  $(\pi/2,0)$ . This fixes  $J = 11.5\text{meV}$ ,  $t_1 = 0.859$ , and  $t_2 = 0.054$  unambiguously and limits the b- to c-axis coupling-ratio to roughly 6% which is consistent with [4-6,13]. While the preceding leaves  $\tilde{\alpha}$ ,  $\delta$ ,  $\beta$ , and  $\mu$  undetermined,  $\tilde{\alpha}$  can be fixed using an additional input, i.e.  $\delta = 0.012$ . This is within the range of values suggested in the literature, i.e.  $\delta = 0.21\dots 0.012$  [11,19,20,22] and implies natural parameters of  $J_1 = 11.4\text{meV} = 132\text{K}$  and  $\tilde{\alpha} = 0.059$ . Allowing for a larger dimerization leads to smaller  $J_1$  and  $\tilde{\alpha}$ . In particular  $\tilde{\alpha} = 0$  with  $J_1 = 124\text{K}$  is reached for  $\delta = 0.076$ . Parameters with a slightly smaller(larger) intra(inter)-chain exchange have been established in [17], i.e.  $J_1 = 9.8\text{meV} = 114\text{K}$ ,  $\tilde{\alpha} = 0$ , and  $t_2 = 0.12$  however with  $\delta = 0.12$ .

The agreement displayed in fig. 6 is satisfying and demonstrates the main point of this section, i.e. that diagonal triplet-hopping can account for the observed asymmetry of the INS data in the D-phase of  $\text{CuGeO}_3$ . Moreover, the values of  $\tilde{\alpha}$  obtained suggests that the intra-chain frustration in  $\text{CuGeO}_3$  is significantly smaller than that derived from the purely 1D  $J_1$ - $\tilde{\alpha}$ - $\delta$  model [19,20], i.e.  $0.24 \gtrsim \tilde{\alpha} \gtrsim 0.36$ . The determination of model parameters however is in need of further studies to improve on the quantitative reliability of the frustration-dependence of presently available approaches for the 2D case. This is in contrast to [17] where *quantitative* evidence for  $\tilde{\alpha} \approx 0$ , based on 3rd-order perturbation theory, has been suggested.

#### D. Dynamic Structure Factor

Magnetic excitations are observed by measuring the dynamic structure factor  $S(\mathbf{q},\omega)$  which is related by an-

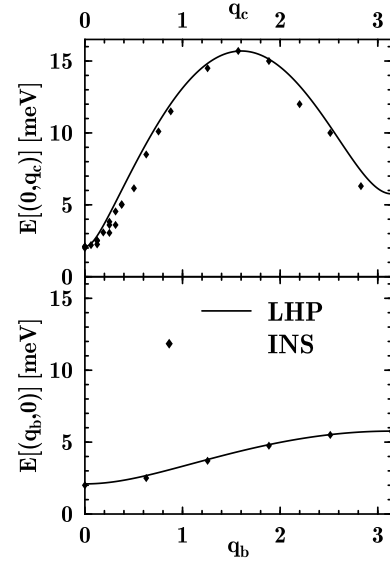


FIG. 6. INS data of c-axis (upper panel) and b-axis (lower panel) dispersion of the triplet mode in the D-phase of  $\text{CuGeO}_3$  at  $T = 1.8\text{K}$  [6] (solid diamonds) versus LHP-theory (solid) for  $J = 11.5\text{meV}$ ,  $t_1 = 0.859$  and  $t_2 = 0.054$ . ( $b = c = 1$ ).

alytic continuation and the fluctuation dissipation theorem  $S(\mathbf{q},\omega) = \text{Im}[\chi(\mathbf{q},\omega)]/(1 - e^{-\omega/T})$  to the dynamic spin susceptibility

$$\chi_{\alpha\beta}(\mathbf{q},\tau) = \langle T_\tau [S_{\mathbf{q}}^\alpha(\tau) S_{\mathbf{q}}^\beta] \rangle . \quad (14)$$

Here  $\mathbf{q}$  is the momentum,  $\tau$  the imaginary time, and  $T_\tau$  refers to time ordering. Since the physical spin is a composite operator of the bond-bosons the information obtained from the dynamic susceptibility is not restricted to the triplet dispersion – even at the LHP level. This will be clarified in the remainder of this section.

Within the LHP representation the spin operator in momentum space is

$$S_{\mathbf{q}}^\alpha = \frac{1}{4}(1 - e^{iq_c})(t_{\mathbf{q}\alpha}^\dagger + t_{-\mathbf{q}\alpha}) - i \frac{1}{4\sqrt{D}}(1 + e^{iq_c}) \sum_{\mathbf{k} \in \mathcal{B}} \varepsilon_{\alpha\beta\gamma} t_{\mathbf{k}+\mathbf{q}\beta}^\dagger t_{\mathbf{k}\gamma} . \quad (15)$$

Two qualitatively different excitations appear on the rhs.: a sharp triplet mode due to the first term and a continuum of two-triplet states due to the second. The momentum dependent form factors  $(1 \mp \exp(iq_c))$  lead to a vanishing weight of the triplet mode (continuum) at  $q_c = 0$  ( $q_c = \pi$ ). Since  $H_{\text{LHP}}$  does not conserve the bare triplet number, the continuum is divided in between two excitations of different nature, i.e. virtual excitations at energies  $E_{\mathbf{k}+\mathbf{q}} + E_{\mathbf{k}}$  and real excitations at energies  $E_{\mathbf{k}+\mathbf{q}} - E_{\mathbf{k}}$ . While the former are due to ground-state quantum-fluctuations and occur at all temperatures, the latter result from excitations across the spin gap and are

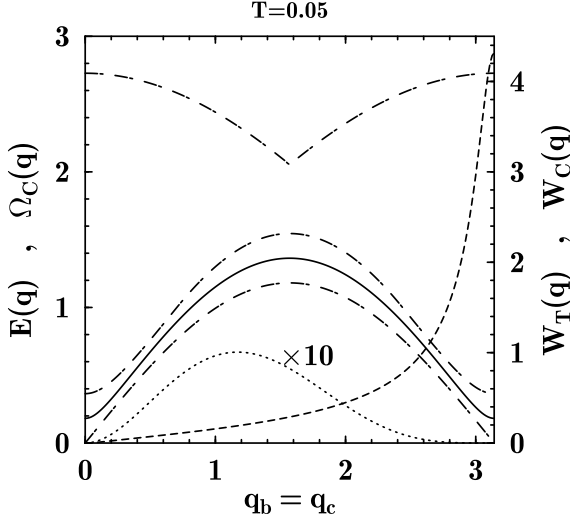


FIG. 7. Energy bounds,  $\Omega_C(\mathbf{q})$ , for both triplet continua (dashed dotted) versus triplet-mode energy,  $E(\mathbf{q})$ , (solid) as well as combined spectral weight of continua,  $W_C(\mathbf{q})$ , (dotted) at  $T = 0.05$  versus spectral weight of triplet mode,  $W_T(\mathbf{q})$ , (dashed) for momenta along  $q_b = q_c$ . ( $b = c = 1$ ,  $J = 1$  and  $t_1, t_2$  as in fig. 6.)

present only at finite temperatures. Evaluating the dynamic susceptibility by standard methods I obtain

$$\begin{aligned} \chi_{\alpha\beta}(\mathbf{q}, \omega_n) = & \delta_{\alpha\beta} \frac{1}{4} \left\{ (\cos(q_c) - 1) \frac{1}{(i\omega_n)^2 - E_{\mathbf{q}}^2} \right. \\ & + (\cos(q_c) + 1) \frac{1}{2D} \sum_{\mathbf{k} \in \mathcal{B}} \left[ \frac{1 + \epsilon_{\mathbf{k}+\mathbf{q}} + \epsilon_{\mathbf{k}} + E_{\mathbf{k}+\mathbf{q}} E_{\mathbf{k}}}{E_{\mathbf{k}+\mathbf{q}} E_{\mathbf{k}}} \times \right. \\ & \quad \left. \frac{n(E_{\mathbf{k}+\mathbf{q}}) - n(E_{\mathbf{k}})}{i\omega_n + E_{\mathbf{k}+\mathbf{q}} - E_{\mathbf{k}}} \right. \\ & \quad \left. + \frac{(1 + \epsilon_{\mathbf{k}+\mathbf{q}} + \epsilon_{\mathbf{k}} - E_{\mathbf{k}+\mathbf{q}} E_{\mathbf{k}})(E_{\mathbf{k}+\mathbf{q}} + E_{\mathbf{k}})}{E_{\mathbf{k}+\mathbf{q}} E_{\mathbf{k}}} \times \right. \\ & \quad \left. \left. \frac{n(E_{\mathbf{k}+\mathbf{q}}) + n(E_{\mathbf{k}}) + 1}{(i\omega_n)^2 - (E_{\mathbf{k}+\mathbf{q}} + E_{\mathbf{k}})^2} \right] \right\}, \quad (16) \end{aligned}$$

where  $\omega_n = 2n\pi T$  is a Bose Matsubara-frequency.

As anticipated the dynamical susceptibility (16) exhibits finite spectral intensity at  $E_{\mathbf{k}}$ ,  $E_{\mathbf{k}+\mathbf{q}} - E_{\mathbf{k}}$ , and  $E_{\mathbf{k}+\mathbf{q}} + E_{\mathbf{k}}$ . This is summarized in fig. 7 which displays the two continua with respect to the triplet mode along a particular momentum space direction. Parameters identical to those of fig. 6 have been chosen. The triplet mode is situated in a gap between the low-energy continuum due to thermal excitations and that at high energies due to quantum fluctuations. At the zone center the latter is gaped by  $2\Delta$ . This is consistent with recent INS data from the D-phase of  $\text{CuGeO}_3$  [24]. In addition to the magnon these experiments indicate an 'unexpected' high-energy continuum which is separated from the magnon by an additional gap. The observed zone-center continuum-to-magnon gap-ratio is approximately

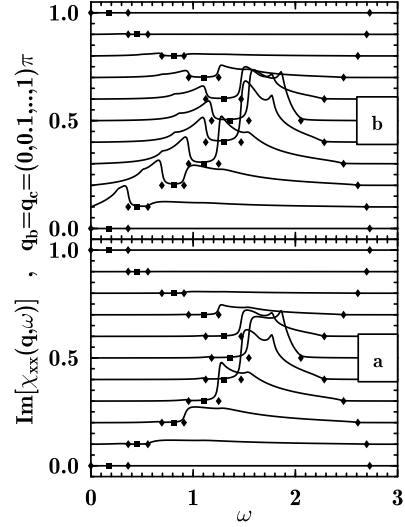


FIG. 8. Triplet continua for various momenta along  $q_b = q_c$  and for two temperatures  $T = 0.05$  (a) and  $T = 0.15$  (b). Bottom-most curve corresponds to  $\mathbf{q} = 0$  with 0.1 incremental y-axis offset for each consecutive momentum. Solid diamonds: bounds of triplet continua. Solid square: triplet-mode energy. ( $b = c = 1$ ,  $J = 1$  and  $t_1, t_2$  as in fig. 6.)

2. Deviations from the latter value of 2 are possibly due to triplet-triplet interactions which are beyond the LHP approach. Additionally, fig. 7 shows the weight of the triplet mode, as well as that of the combined continua at  $T = 0.05J$ . At  $T \ll J$  the continuum weight is almost completely due to quantum fluctuations while, independent of temperature, the triplet weight is given by

$$W_T(\mathbf{q}) = \frac{\pi}{8} \frac{1 - \cos(q_c)}{E_{\mathbf{q}}} \stackrel{(\pi, \pi)}{=} \frac{\pi}{4\Delta}, \quad (17)$$

The leftmost expression refers to the maximum of the triplet weight. The corresponding momentum, i.e.  $(\pi, \pi)$ , indicates the instability towards AMF as  $\Delta \rightarrow 0$ .

Figure 8 depicts the spectral intensity  $\text{Im}[\chi_{xx}(\mathbf{q}, \omega_n \rightarrow -i\omega + \nu)]$  of the continua as a function of frequency for two temperatures and for various momenta along a direction in reciprocal space identical to that of fig. 7. The  $\mathbf{k}$ -sums of (16) have been performed numerically on a  $600 \times 300$  lattice. In order to obtain sufficient smoothing the frequency has been shifted off the real axis by  $\nu = 0.05$ . The parameters correspond to those of fig. 6. As a guide to the eye the position of the triplet mode is labeled by solid squares while solid diamonds in this figure label the exact locations of the spectral bounds of the continua. Although smeared due to the imaginary broadening, van-Hove singularities are clearly observable at the spectral bounds as well as other characteristic energies within the continua. Evidently the quantum fluctuations exhibit largest weight at intermediate wave vectors while at higher temperatures additional weight appears at smaller momentum due to thermal excitations. Even though the intensity in fig. 8 decreases both, as  $\mathbf{q}$  ap-

proaches (0,0) and  $(\pi, \pi)$ , only in the latter case this is due to the form factor in (15) while in the former case this is a consequence of the conservation of the total spin.

#### IV. CONCLUSION

In summary I have studied static and dynamic properties of a frustrated and dimerized 2D quantum spin-model using the bond-operator method. The ground state energy and the spin gap have been gauged against known results from the 1D limiting cases of this model. Effects of dimerization are found to be described almost quantitatively while the influence of frustration is captured qualitatively. The dynamic structure factor has been analyzed and displays two characteristic features, i.e. a well defined magnon excitation and a temperature dependent continuum. The magnon dispersion shows a characteristic lifting of degeneracies, different from purely one-dimensional models, and agrees very well with INS data on  $\text{CuGeO}_3$ . The low-temperature continuum exhibits a zone-center gap twice that of the magnon. This is also consistent with INS experiments on  $\text{CuGeO}_3$ .

#### ACKNOWLEDGMENTS

I am grateful to P. Fulde and the Max-Planck-Institut für Physik komplexer Systeme for their kind hospitality. It is a pleasure to thank G. Uhrig for helpful comments and for communicating his results prior to publication. Stimulating discussions with B. Büchner and E. Müller-Hartmann are acknowledged. This work has been supported in part by the Deutsche Forschungsgemeinschaft through the SFB 341.

#### APPENDIX A: BOND-OPERATOR MEAN-FIELD THEORY (MFT)

An alternative approach to the Hamiltonian (5) arises by introduction of a set of local Lagrange multipliers  $\eta$  to enforce the constraint (3)

$$\tilde{H} = H - \sum_{\mathbf{l} \in \mathcal{D}} \eta (\mathbf{s}_1^\dagger \mathbf{s}_1 + \mathbf{t}_{1\alpha}^\dagger \mathbf{t}_{1\alpha} - 1) \quad . \quad (\text{A1})$$

To treat this Hamiltonian one replaces the local constraint by a global one, i.e.  $\eta = \eta$ , and introduces a mean-field (MF) decoupling of all quartic terms leading to an effective quadratic Hamiltonian [27]. This Hamiltonian has an overall *negative* prefactor to the  $\mathbf{s}_1^\dagger \mathbf{s}_1$ -term which implies Bose condensation of the singlets. Therefore  $\mathbf{s}_1^\dagger = \mathbf{s}_1 = \langle \mathbf{s}_1 \rangle = \mathbf{s}$  is assumed. Moreover it can be shown that contributions from the triplic and quartic triplet-terms  $H_2$  and  $H_3$  to the MFT can be neglected [40,41]. The MF Hamiltonian reads

$$H_{MFT} = D \left( -\frac{3}{8} - \frac{3}{4} s^2 - \eta s^2 + \frac{5}{2} \eta \right) + \frac{1}{2} \sum_{\mathbf{k} \in \mathcal{B}} \Psi_{\mathbf{k}\alpha}^\dagger \begin{bmatrix} \frac{1}{4} - \eta + s^2 \epsilon_{\mathbf{k}} & s^2 \epsilon_{\mathbf{k}} \\ s^2 \epsilon_{\mathbf{k}} & \frac{1}{4} - \eta + s^2 \epsilon_{\mathbf{k}} \end{bmatrix} \Psi_{\mathbf{k}\alpha} \quad , \quad (\text{A2})$$

with notations equivalent to (7). Analogous to the latter equation (A2) represents three dispersive triplet excitations, however, with a modified dispersion relation. After a Bogoliubov transformation one gets [42]

$$H_{MFT} = D \left( -\frac{3}{8} - \frac{3}{4} s^2 - \eta s^2 + \frac{5}{2} \eta \right) + \sum_{\mathbf{k} \in \mathcal{B}, \alpha} E_{\mathbf{k}}^{MFT} (b_{\mathbf{k}\alpha}^\dagger b_{\mathbf{k}\alpha} + \frac{1}{2}) \quad (\text{A3})$$

$$E_{\mathbf{k}}^{MFT} = \left( \frac{1}{4} - \eta \right) \sqrt{1 + d \epsilon_{\mathbf{k}}} \quad , \quad (\text{A4})$$

where  $d = 2s^2/(1/4 - \eta)$ . The  $b_{\mathbf{k}\alpha}$  quasi-particles follow from expressions identical to (11) with  $\epsilon_{\mathbf{k}}$ ,  $1 + \epsilon_{\mathbf{k}}$ , and  $E_{\mathbf{k}}$  replaced by  $s^2 \epsilon_{\mathbf{k}}$ ,  $\frac{1}{4} - \eta + s^2 \epsilon_{\mathbf{k}}$ , and  $E_{\mathbf{k}}^{MFT}$ , respectively. The Lagrange multiplier and the singlet amplitude have to be determined by solving the saddle-point equations  $\langle \partial H_{MFT} / \partial \eta \rangle = 0$  and  $\langle \partial H_{MFT} / \partial s \rangle = 0$ . This leads to

$$0 = s^2 - \frac{2}{5} + \frac{3}{D} \sum_{\mathbf{k} \in \mathcal{B}} \frac{1 + d \epsilon_{\mathbf{k}}/2}{\sqrt{1 + d \epsilon_{\mathbf{k}}}} (\langle b_{\mathbf{k}x}^\dagger b_{\mathbf{k}x} \rangle + \frac{1}{2}) \quad (\text{A5})$$

$$0 = \frac{3}{4} + \eta - \frac{3}{D} \sum_{\mathbf{k} \in \mathcal{B}} \frac{\epsilon_{\mathbf{k}}}{\sqrt{1 + d \epsilon_{\mathbf{k}}}} (\langle b_{\mathbf{k}x}^\dagger b_{\mathbf{k}x} \rangle + \frac{1}{2}) \quad . \quad (\text{A6})$$

These selfconsistency equations can be solved by combining them into a single one for the variable  $d$  only

$$d = 5 - \frac{3}{D} \sum_{\mathbf{k} \in \mathcal{B}} \frac{2}{\sqrt{1 + d \epsilon_{\mathbf{k}}}} (\langle b_{\mathbf{k}x}^\dagger b_{\mathbf{k}x} \rangle + \frac{1}{2}) \quad (\text{A7})$$

$$\stackrel{(T=0)}{=} 5 - \frac{3}{D} \sum_{\mathbf{k} \in \mathcal{B}} \frac{1}{\sqrt{1 + d \epsilon_{\mathbf{k}}}} \quad , \quad (\text{A8})$$

where  $\eta$  follows by insertion of  $d$  into (A6). This completes the description of the bond-operator MFT.

- 
- [1] M. Hase *et al.*, Phys. Rev. Lett. **70**, 3651 (1993)
  - [2] M. Isobe and Y. Ueda, J. Phys. Soc. Japan **65**, 1178 (1996)
  - [3] M. Weiden *et al.*, preprint, cond-mat/9703052
  - [4] M. Nishi *et al.*, Phys. Rev. B **50**, 6508 (1994)
  - [5] L.P. Regnault *et al.*, Physica B **213** & **214**, 278 (1995)
  - [6] L. P. Regnault, *et al.*, Phys. Rev. B **53**, 5579 (1996)
  - [7] M.C. Martin *et al.*, Phys. Rev. B **53**, R14713 (1996)
  - [8] J.P. Pouget *et al.*, Phys. Rev. Lett. **72**, 4037 (1994); O. Kamimura *et al.*, J. Phys. Soc. Jpn. **63**, 2467 (1994); S.B. Oseroff *et al.*, Phys. Rev. Lett. **74**, 1450 (1995)

- [9] H. Völlenkle *et al.*, Monatsh. Chem. **98**, 1352 (1967); G.A. Petrakovskii *et al.*, Zh. Eksp. Teor. Fiz. **98**, 1382 (1990) [Sov. Phys. JETP **71**, 772 (1990)]; J.E. Lorenzo *et al.*, Phys. Rev. B **50**, 1278 (1994); Q.J. Harris *et al.*, Phys. Rev. B **50**, 12606 (1994); M. Arai *et al.*, J. Phys. Soc. Jpn. **63**, 1661 (1994)
- [10] K. Hirota *et al.*, Phys. Rev. Lett. **73**, 736 (1994);
- [11] M. Braden *et al.*, Phys. Rev. B **54**, 1105 (1996)
- [12] W. Geertsma and D. Khomskii, Phys. Rev. B **54**, 3011 (1996)
- [13] D. Khomskii, W. Geertsma, and M. Mostovoy, Czech. J. Phys. **46**, Suppl. 6, 3239 (1996)
- [14] H. Kuroe *et al.*, Phys. Rev. B **50**, 16468 (1994)
- [15] P.H.M. van Loosdrecht *et al.*, Phys. Rev. Lett. **76**, 311 (1996)
- [16] P. Lemmens *et al.*, Physica B **223&224**, 535 (1996)
- [17] G. Uhrig, preprint, (1997).
- [18] Y. Fujii *et al.*, J. Phys. Soc. Japan **66**, 326 (1997)
- [19] G. Castillia *et al.*, Phys. Rev. Lett. **75**, 1823 (1995)
- [20] J. Riera *et al.*, Phys. Rev. B **51**, 16098 (1995)
- [21] K. Okamoto and K. Nomura, Phys. Lett. A **169**, 433 (1992)
- [22] S. Haas *et al.*, Phys. Rev. B **52**, R14396 (1995); G. Bouzerar *et al.*, preprint, cond-mat/9701176
- [23] M. Arai *et al.*, Phys. Rev. Lett. **77**, 3649 (1996)
- [24] M. Ain *et al.*, Phys. Rev. Lett. **78**, 1560 (1997)
- [25] G.S. Uhrig and H.J. Schulz, Phys. Rev. B **54**, R9624 (1996)
- [26] A. Fledderjohann and C. Gros, Europhysics Lett. **37**, 189 (1997)
- [27] S. Sachdev and R. N. Bhatt, Phys. Rev. B **41**, 9323 (1990)
- [28] O. A. Starykh *et al.*, Phys. Rev. Lett. **77**, 2558 (1996)
- [29] A. V. Chubukov, Pis'ma Zh. Eksp. Teor. Fiz. **49**, 108 (1989) [JETP Lett. **49**, 129 (1989)]
- [30] A. V. Chubukov and Th. Jolicoeur, Phys. Rev. B **44**, 12050 (1991)
- [31] Z. G. Soos, S. Kuwajima, and J. E. Mihalick, Phys. Rev. B **32**, 3124 (1985)
- [32] T. Tonegawa and I. Harada, J. Phys. Soc. Jpn. **56**, 2153 (1987).
- [33] R. Chitra *et al.*, Phys. Rev. B **52**, 6581 (1995)
- [34] A. Brooks Harris, Phys. Rev. B **7**, 3166 (1973); see also: M. Reigrotzki, H. Tsunetsugu, and T.M. Rice, J. Phys.: Condens. Matter **6**, 9235 (1994)
- [35] 3rd-order perturbation theory displays a shallow minimum at  $\tilde{\alpha} \approx 0.11$
- [36] S. R. White and I. Affleck, Phys. Rev. B **54**, 9862 (1996)
- [37] A similar observation has been made by: Jun Zang, A.R. Bishop, and D. Schmeltzer Phys. Rev. B **52**, 6723, (1995).
- [38] On a smaller scale this also applies to 3rd-order perturbation theory.
- [39] This is possibly due to different extrapolation procedures and due to different numbers of states kept per block, K. Hallberg and K. Penc, private communication.
- [40] S. Gopalan, T. M. Rice, and M. Sigrist, Phys. Rev. B **49**, 8901 (1994)
- [41] W. Brenig, unpublished
- [42]  $\eta < 1/4$  is assumed and selfconsistently satisfied.